

中国激光

基于非线性环形放大镜和微纳光纤锁模激光器的研究现状

张海涛^{*}, 邓德才, 李宇航^{**}, 祖嘉琦, 陈俊宇, 巩马理, 柳强

清华大学精密仪器系激光与光子技术研究室, 光子测控技术教育部重点实验室, 北京 100084

摘要 被动锁模光纤激光器是超快激光家族中的重要成员,凭借光纤的优良特性,如鲁棒性好、结构简单紧凑、稳定可靠等,吸引了相关研究者的广泛关注。近年来,随着光纤制备工艺和锁模技术的不断进步,光纤锁模激光器得到了迅速发展。基于此,描述锁模技术及不同色散区的锁模激光器,并依据锁模机制、脉冲性质等分类叙述,综述了国内外该领域的研究现状和发展趋势,重点阐述全光纤非线性环形放大镜和微纳光纤锁模激光器的研究进展。

关键词 激光技术; 光纤锁模激光器; 非线性环形放大镜; 微纳光纤; 耗散孤子; 脉动孤子

中图分类号 TN248

文献标志码 A

doi: 10.3788/CJL202148.1501006

1 引言

光纤激光器得益于光纤结构的固有属性,有着其他激光器不可比拟的优势,比如单程增益高、光光效率高、鲁棒性好、可弯折、免光路交接等,受到了国际上研究者们的广泛关注。锁模光纤振荡器作为光纤激光领域中最前沿、最活跃的分支之一,最早的研究可以追溯至 1983 年,Dzhibladze 等^[1]在掺钕光纤激光器中首次观察到了局部锁模现象。1990 年,改进的被动锁模光纤激光器实现了飞秒量级的激光脉冲输出^[2]。锁模技术的出现开辟了超快激光的新时代,实现锁模的器件主要有两大类,一种为主动锁模器件,比如电光、声光、磁光调制器,另一种为被动锁模器件,多是采用可饱和吸收体或等效的可饱和吸收体。主动锁模通过在腔内引入周期性的损耗,并且调制频率同于纵模间隔频率,实现对脉冲振幅的调制,从而实现对各个纵模的锁相。这种锁模方式可与外部电脉冲信号合成,重复频率可调谐,并且易获得高重复频率光脉冲序列,被广泛应用于光纤通信领域,但是输出脉冲的光谱宽度一般为几纳米,因而所能实现的最窄脉宽有限,仅为 ps 量级。被动锁模利用可饱和吸收作用,相比于主动锁模,可饱和吸

收体有着更短的响应时间,调制前后沿更为陡峭,所能实现的脉冲宽度更窄;此外,避免了复杂的光学调制器,整体结构更简洁,锁模状态更加稳定,是目前实现飞秒脉冲激光器的首选方案。随后的几十年里,被动锁模光纤激光器不断推陈出新,在提升脉冲能量和功率方向上,研究者们不断探索新型锁模方式和激光材料,各种锁模理论、技术被不断提出,如色散管理锁模、自相似锁模、全正色散锁模、耗散孤子共振、Mamyshev 锁模^[3]等。在稳定性方向,一方面各种非稳态锁模状态被发现和合理规避,并凭借色散傅里叶变换技术,具有非稳态现象的非线性动力学过程得以记录和研究。另一方面锁模光纤激光器也逐渐地趋向于全光纤化和小型化,基于非线性环形放大镜(NALM)锁模的振荡器在这方面表现更为突出。另外伴随着光纤制造技术的进步,基于微结构的光纤锁模振荡器也发展迅速,为传统锁模方式注入了新的活力。时至今日,被动锁模光纤激光理论和技术基本完善,主要研究工作主要围绕新锁模材料和器件的开发使用、锁模光纤激光器的应用、输出能量的提升、脉冲宽度的压缩、全光纤化和实用化等。

基于此,本文将介绍各种锁模技术的发展现状和趋势,重点介绍全光纤结构 NALM 锁模和微纳

收稿日期: 2021-03-31; 修回日期: 2021-04-30; 录用日期: 2021-05-11

基金项目: 国家自然科学基金(61475081)

通信作者: *zhanghaitao@mail.tsinghua.edu.cn; **liyuhang@tsinghua.edu.cn

光纤锁模。

2 被动锁模光纤激光器的发展

被动锁模激光器的典型原理结构如图 1 所示。被动锁模器件是锁模激光器自启动的关键,可以是可饱和吸收体(SA),也可以是非线性偏振演化(NPE)的等效可饱和吸收体。对于 SA,最常用的结构为半导体可饱和吸收镜(SESAM),关于 SESAM 的研究最早可追溯至 1990 年^[4],经过数十年的迭代发展,已成为商业上最为成熟的锁模器件,许多产品被应用于科学研究^[5-7]。但是 SESAM 本身的损伤阈值较低,寿命较短,为此研究者也在不断探索新型可饱和吸收材料。在过去十多年中,使用新型可饱和吸收体实现锁模的研究被不断报道,例如碳纳米管^[8]、石墨烯^[9]、钙钛矿薄膜^[10]、过渡金属二卤化物^[11]及拓扑材料^[12],均取得了不错的锁模结果,但是整体而言,此类材料所能实现的能量普遍比等效可饱和吸收体低。

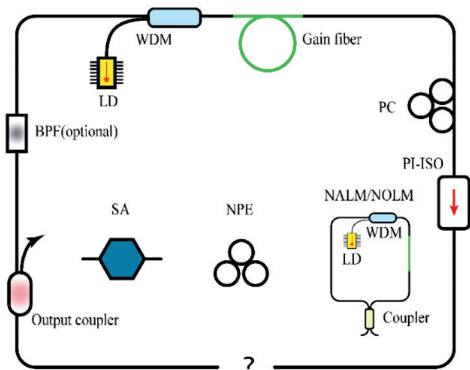


图 1 典型的被动锁模光纤振荡器结构示意图

Fig. 1 Schematic of typical passive mode-locked fiber oscillator

对于等效可饱和吸收体,通常利用光纤中的非线性效应,配合使用特定的光学器件实现等效的可饱和吸收效应。比如,腔内的非线性偏振演化效应结合偏振相关隔离器形成的等效可饱和吸收体实现的锁模,通常称为 NPE 锁模^[13]。椭圆偏振的激光脉冲在光纤内传输时,非线性偏振演化,致使时域脉冲的不同部分(如波峰、波腹、波谷)具有不同的极化状态,然后配合使用偏振相关隔离器,使得波峰的透射率高于波谷,从而实现对脉冲振幅和宽度的调制。NPE 锁模一般会引入空间结构或添加偏振控制器,不易集成全光纤,环境可靠性略差。另一种等效可饱和吸收体通过光纤耦合器与激光腔相连的光纤副环路,可实现全光纤化,稳定可靠,典型的结构包括非线性光学环形镜(NOLM)^[14]和 NALM^[15-17]。腔

内脉冲在进入副环路时被耦合器分成两个相向传播方向的脉冲。对于 NOLM 而言,两路的初始脉冲强度一般相差较大,经过副环后积累的非线性相移不同,再次通过耦合器返回激光腔时发生干涉,配合腔内的隔离器实现了对脉冲振幅的调制。想要实现可饱和吸收效果,需要合理设计 NOLM 的长度和耦合器的分束比。NALM 环在 NOLM 环的基础上,在副环路中增加一级光放大器,通过改变放大器的放大效果,实现对两路脉冲非线性相移差异的调控,有着更多的调节自由度,更容易实现锁模的自启动。

由于光纤本身属性,超短光脉冲传输时,除了存在色散效应,还会受到非线性效应的调控,如自相位调制(SPM)效应、交叉相位调制(XPM)及受激拉曼散射(SRS)等。色散与非线性均会对脉冲的相位进行调制,因而腔内不同色散分布下的脉冲演化会有差异,锁模机制也不相同。根据腔内色散和色散管理,锁模光纤激光器可以分为 4 大类,分别是传统孤子锁模^[18]、色散管理孤子锁模(也称呼吸孤子锁模)^[19]、自相似锁模^[20]、耗散孤子锁模^[21]。

传统孤子锁模振荡器最早报道于 1981 年^[22],腔内光纤全部为负色散,因而光脉冲在传输过程中的群速度色散(GVD)会赋予脉冲负啁啾,即脉冲的瞬时频率随时间逐渐降低,同时受到 SPM 的作用,在脉冲波峰附近形成正啁啾。在腔内 GVD 和 SPM 的共同作用下,脉冲达到平衡,在腔内稳定传输且不带啁啾,直接输出飞秒脉冲^[23]。传统孤子锁模输出的脉冲能量受孤子面积定理约束^[24],在光纤纤芯面积一定的前提下,传统孤子锁模振荡器的输出脉冲能量十分有限,一般来说,使用单模光纤的锁模激光器的脉冲能量只能达到~100 pJ 数量级^[25-26]。

色散管理孤子锁模^[27-28]与传统孤子锁模激光器不同,腔内的总色散量接近 0 ps²,并且脉冲在腔内传播时的脉宽并非保持不变,而是在腔内正负色散介质的作用下分别展宽和窄化。脉冲展宽和窄化的过程中,等效的脉冲平均脉宽更宽,可以降低非线性效应的积累,获得更高的单脉冲能量,实现 nJ 量级脉冲的输出^[29-31]。但是继续提升脉冲能量时,仍会出现诱导锁模的不稳定造成多脉冲的现象^[32]。

1993 年,Anderson 等^[33]发现具有线性啁啾的抛物线形脉冲能够在正色散区域实现无光波分裂的传输。接着 Ilday 等^[20]提出了自相似锁模理论。自相似孤子在激光器腔内传输时,可以承受更强的非线性效应而不会发生脉冲分裂,脉冲形状和线性啁

啾量在传输时保持不变,而脉冲能量、光谱宽度和峰值功率则呈指数增长。自相似孤子锁模能够实现大于 10 nJ 的单脉冲能量输出^[34]。但是由于增益介质本身的增益带宽有限,当脉冲的光谱宽度超过增益带宽时,自相似演化过程就会终止^[35],同时也会受到高阶色散效应和 SRS 的限制^[36]。这些因素成为了自相似锁模振荡器能量提升的壁垒。

2006 年,Chong 等^[37]提出了耗散孤子锁模,在全正色散介质腔内,通过引入光谱滤波机制实现自启动锁模,无需色散管理,易光纤化,大大地提高了振荡器的可集成性。耗散孤子与传统孤子不同,由于正群速度色散与自相位调制对脉冲均引入正啁啾信息,无法实现平衡收敛,因而需要群速度色散、自相位调制、增益、损耗、光谱滤波的共同作用,依赖能量在系统内不断地输入输出实现动态平衡,这也正是“耗散孤子”意义所在^[38]。由于腔内正色散量较大,耗散孤子一般具有强啁啾,脉宽显著展宽,因此可以容忍更强的非线性效应而不分裂,实现大能量的脉冲输出,是高能量锁模光纤振荡器发展的一个重要里程碑。2007 年,Chong 等^[39]通过优化腔内光谱滤波效果,实现了单脉冲能量超过 20 nJ,压缩后脉冲宽度小于 200 fs 的输出结果。然而,超过 10π 以上的非线性相移累积仍然会造成脉冲的分裂^[40-41]。为了避免脉冲分裂,2008 年,Chang 等^[42]依据复三次-五次金兹伯格朗道方程(CQGLE)预测了一种新型孤子,耗散孤子共振(DSR)。该孤子利用可饱和逆吸收区域的峰值功率钳制效应,脉冲宽度随泵浦强度单调增加,而脉冲峰值功率保持恒定,理论上可以实现无限高的能量而不发生脉冲分裂。大量的理论和实验研究结果表明:耗散孤子共振的实现不依赖于锁模技术和色散符号,使用 NPE^[43-45]、

8 字腔^[46-48]、SA^[49-50]等锁模技术,在正常或反常色散区域均可实现耗散孤子共振锁模^[51-52]。

近几年,研究者们探索出了一种新型的振荡器,即 Mamyshev 振荡器^[53],能突破上述锁模机制的许多限制,如图 2(a)所示,它可以看出两个串联的 Mamyshev 再生器。脉冲在其中传输时,受 SPM 作用光谱展宽,接着通过中心波长偏离具有脉冲波长的带通滤波器。此滤波器仅允许 SPM 诱导产生的光谱分量通过,低强度脉冲因非线性相移不足而被滤除,利用该滤波机制可以实现等效的可饱和吸收体^[54]。Mamyshev 振荡器的输出性能很大程度上取决于两个滤波器中心波长的偏离程度,大间隔往往需要更大的光谱展宽,同时可允许更高能量、更宽谱宽的脉冲进行传输。比如,Frank Wise 课题组采用如图 2(b)所示的结构,在约 10 nm 的间隔下观察到高达 60π 的非线性相移,所获脉冲的峰值功率高达兆瓦量级、光谱宽度超过 100 nm^[55]。2019 年,天津大学胡明列课题组^[56]报道的 Mamyshev 锁模激光振荡器,实现了单脉冲能量为 1 μ J,脉冲宽度为 41 fs,峰值功率为 13 MW 的输出结果,获得了目前光纤锁模振荡器所能实现的最高能量和最高平均功率。可以看出:Mamyshev 锁模机制在实现高能量、宽光谱、窄脉宽输出方面有着天然优势;此外,Mamyshev 振荡器也可以全光纤集成,具有良好的环境鲁棒性^[57]。然而,这种高效的可饱和吸收效应使得锁模自启动成为问题。目前,研究者们提出了多种锁模启动的方式,其中包括自发辐射放大反馈技术^[58]、泵浦调制技术^[57]、辅助腔技术^[59],均是向空腔中引入一个短暂合适的脉冲波动,使其逐步演化为稳定的锁模脉冲,虽然无需外部激励,但是与前述的锁模振荡器相比,自启动难度仍相对较大。

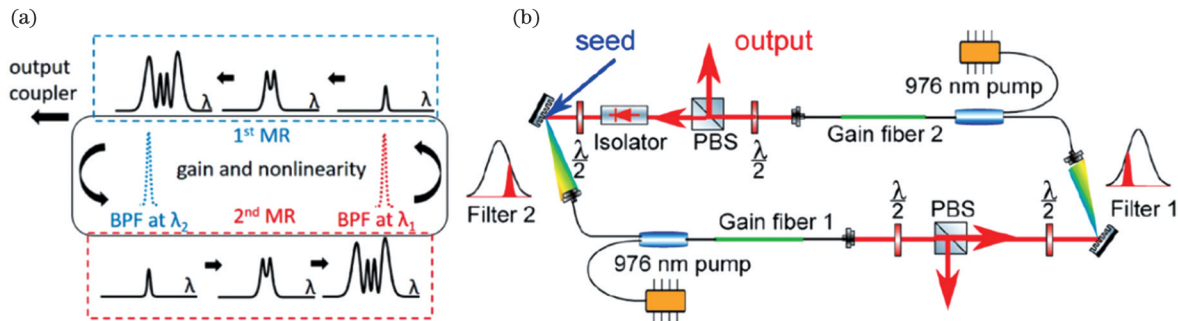


图 2 Mamyshev 振荡器。(a) Mamyshev 振荡器原理示意图^[53]; (b) 具有 MW 峰值功率的 Mamyshev 振荡器示意图^[55]
Fig. 2 Mamyshev oscillator. (a) Schematic of the principle of Mamyshev oscillator^[53]; (b) schematic of Mamyshev oscillator with MW-order peak power^[55]

在锁模状态启动和控制的方向上,研究者们也开始尝试结合人工智能方式。2016 年,Woodward

等^[60]在 NALM 锁模激光器的基础上,通过遗传算法控制 NALM 中的偏振,实现了一台智能激光器。

该激光器能够在多参数空间中自优化快速探索出最优解，并在存在外部干扰的情况下，始终定位于全局最优值。2019 年，Pu 等^[61]基于实时类人算法，实现了智能锁模光纤激光器。该激光器可以自动锁定在不同的锁模状态，包括基本锁模、谐波锁模、调 Q 和调 Q 锁模，而不需要任何物理结构的改变，同时也可以在环境干扰引起的失锁状态下迅速恢复。人工智能激光器结合了人的方法和计算机的计算能力、速度和精度，而算法是此类激光器的关键。未来随着激光器各个参数更加精确的量化方式和算法的迭代优化，此类智能锁模激光器有着广阔的发展前景。

除脉冲能量、宽度等参数，飞秒脉冲的重复频率也是科学和工业应用领域需要关注的重要指标参数，腔长决定了锁模超快光纤振荡器的重复频率。大多数光纤振荡器包括几米长的光纤，典型的重复频率是几十兆赫兹。在谐振腔中加入更长的无源光纤可以降低重复频率。然而，将环腔振荡器的重复频率降低到 1 MHz 以下，对应的谐振腔长度大约为 200 m。这样的长腔有两个缺点：振荡器容易受到

外界干扰，从而破坏锁模状态；输出脉冲产生非线性的巨大啁啾，使脉冲难以压缩。在实际应用中，重复频率低于 10 MHz 的超短脉冲通常由声光调制器进行脉冲拾取获得；重复频率超过 200 MHz 的锁模光纤激光器也具有挑战性；尤其当重复频率超过 1 GHz 时，腔光纤长度需缩短至 10 cm 以下，此时有源光纤必须高度掺杂才能提供足够的增益。2015 年北京大学采用如图 3(a)所示的结构，并使用双端高功率泵浦方式实现高增益，控制整体腔长，实现了重复频率为 1 GHz，光谱 23 nm，傅里叶压缩极限脉冲宽度为 64 fs 的输出结果^[62]。目前光纤锁模激光器所能实现的最高重复频率为 2011 年 Martinez 等^[63]所报道的 19.45 GHz，激光器采用了 5 mm 长的法布里-珀罗腔光纤，结合碳纳米管可饱和吸收结构，输出脉冲宽度为 790 fs。2019 年，北京大学基于同样的方式，在 1 μm 波段实现了 12.5 GHz 重复频率的飞秒锁模光纤激光器^[64]，结构如图 3(b)所示，总腔长为 7.6 mm，在泵浦功率为 130 mW 时即可启动锁模，输出脉宽为 1.9 ps。

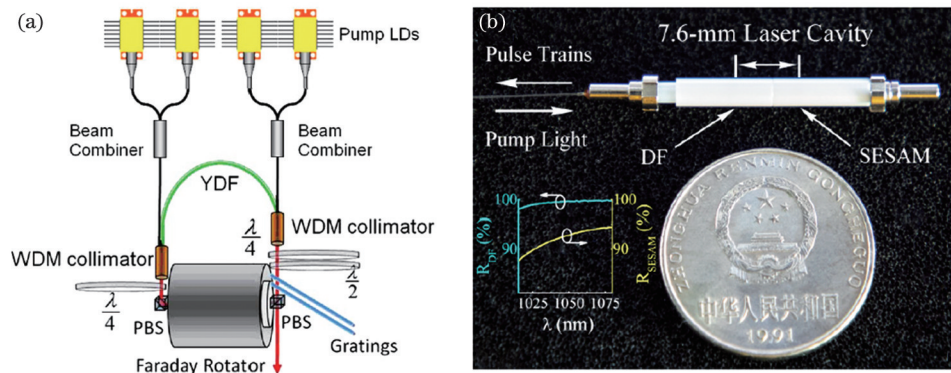


图 3 高重复频率光纤激光器。^(a)1 GHz 重复频率的锁模光纤激光器^[62]；^(b)基于法布里-珀罗腔的锁模光纤激光器，重复频率为 12.5 GHz^[64]

Fig. 3 High repetition rate fiber laser. (a) Mode-locked fiber laser with 1 GHz repetition rate^[62]；(b) mode-locked fiber laser based on Fabry-Perot cavity with repetition rate of 12.5 GHz^[64]

3 基于 NALM 环锁模的全光纤激光器

NALM/NOLM 是一种优异的等效可饱和吸收体，自从 NOLM 环和 NALM 环锁模被提出以来，就凭借固有优势受到广泛研究者们的关注，包括 1 μm 和 1.5 μm 波段^[65-67]。这类振荡器可采用全保偏器件，可以避免锁模对机械结构的依赖，具有长时间的环境稳定性和可靠性，此外，其输出为线偏振光，用作啁啾脉冲放大器(CPA)系统的种子源时，能够实现高效的光栅对压缩。

2012 年，新西兰 Aguergaray 考题组^[68]基于全保偏的 NALM 环锁模结构，实现了重复频率

为 10 MHz，单脉冲能量为 0.3 nJ，脉冲宽度为 344 fs 的输出结果。同年，该课题组通过增加主环路中单模光纤的长度，如图 4(a)所示，降低重复频率以获得大脉冲能量，实现了巨啁啾耗散孤子，最大输出脉冲能量、脉宽与单模光纤长度的关系如图 4(b)所示，可以看出当主环中单模光纤长度增加至 100 m 时，所能实现的最大脉冲能量达 16 nJ，对应振荡器重复频率 1.7 MHz，此时压缩后脉冲宽度为 370 fs^[69]。同时根据图 4(c)可以看出，输出脉冲宽度与单模光纤长度存在线性关系，而且峰值功率基本恒定，也证明了峰值功率的钳制效应。

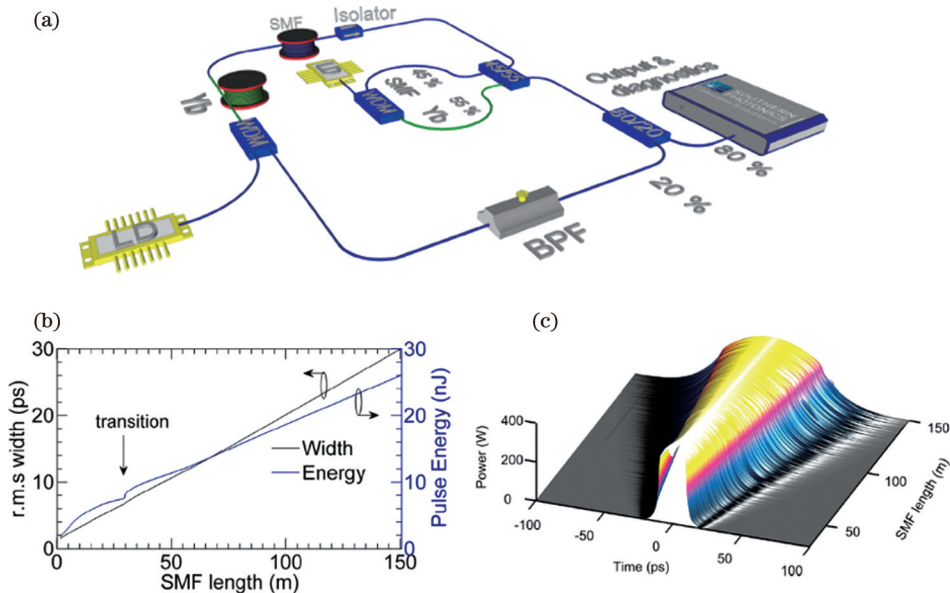


图 4 基于 NALM 环的锁模光纤激光器^[69]。(a)谐振腔示意图;(b)输出能量脉宽与单模光纤长度的关系;
(c)输出波形与单模光纤长度的关系

Fig. 4 Mode-locked fiber laser based on NALM^[69]. (a) Schematic of the resonant cavity; (b) relationship between output energy pulse width and single mode fiber length; (c) relationship between output waveform and single mode fiber length

次年,该团队又通过腔参数的优化,实现了 120 fs、4.2 nJ、10 MHz 的脉冲序列输出^[70]。此外,Zhou 等^[71]在 2015 年同样采用巨啁啾脉冲方案,将能量提升到了 50 nJ,重复频率为 1.44 MHz,然而脉冲宽度较宽,为 750 fs。2016 年,Zhou 等^[72]又报道了 32 nJ 单脉冲能量,615 fs 脉宽,1.44 MHz 重复频率的成果。2016 年,Kuse 等^[73]研究结果表明在 NALM 环中附加相位偏置,利于该类激光器的锁模自启动,并基于此搭建了高稳定的光学频率梳。

清华大学在 2018 年搭建的基于 NALM 环锁模的全保偏光纤激光器^[74]如图 5(a)所示,整体腔长为 20 m,重复频率为 8.02 MHz。测试了输出功率与泵浦功率的关系,如图 5(b)所示,最高可实现 60 mW 的平均功率输出,对应单脉冲能量为 7.5 nJ,腔外脉冲宽度可以压缩至 200 fs,同时在此状态下测量了 4 h 的功率稳定性,结果表明功率波动仅为 0.07%,意味着此激光器具有非常高的稳定性。

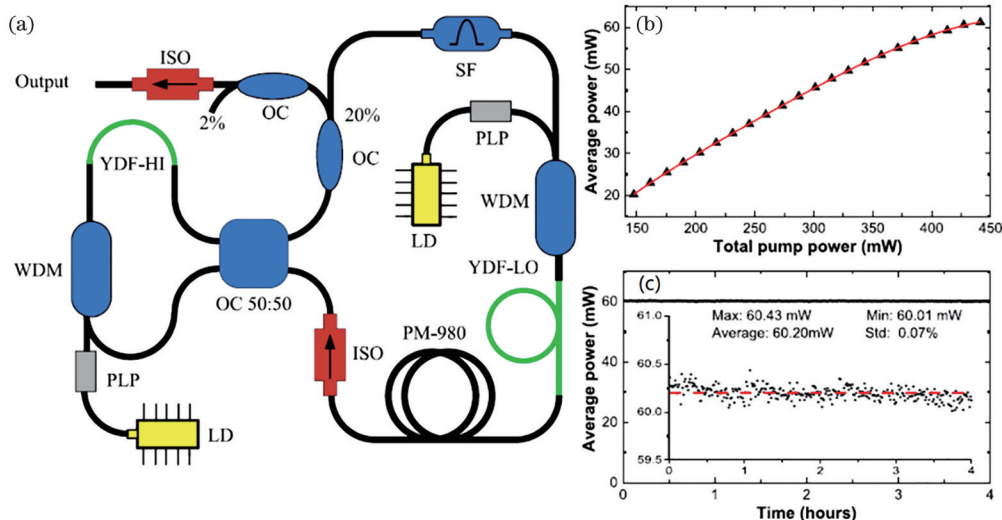


图 5 高平均功率 NALM 环振荡器^[74]。(a)全保偏 NALM 环锁模光纤激光器结构示意图;(b)平均功率和泵浦功率的关系;
(c)4 h 功率稳定性

Fig. 5 High average power fiber laser with NALM^[74]. (a) Schematic of all-polarization-maintaining mode-locked fiber laser with NALM; (b) relationship between average power and pump power; (c) power stability over 4 h

2018 年, Yu 等^[75]通过优化腔内单模光纤长度的分布,实现了单脉冲能量为 10 nJ,脉冲宽度为 93 fs,重复频率为 6 MHz 的输出结果。2020 年,北京工业大学^[76]在重复频率 100 kHz 下,实现了单脉冲能量为 104 nJ 的结果,但是压缩后脉宽仅为 1.053 ps。可以看出,巨啁啾方案可以实现更高的单脉冲能量,但是需要牺牲压缩脉冲宽度,脉冲宽度通常大于 200 fs,而且在高能量下长腔的引入更易引起锁模的不稳定性^[77],继而诱发脉冲分裂,甚至会进入类噪声锁模区域^[78-79],限制了巨啁啾方案单脉冲能量的进一步提升。因此,研究如何在特定的腔长下提升 NALM 环锁模的输出性能很有必要。

2020 年,清华大学^[17]通过理论和实验探索了

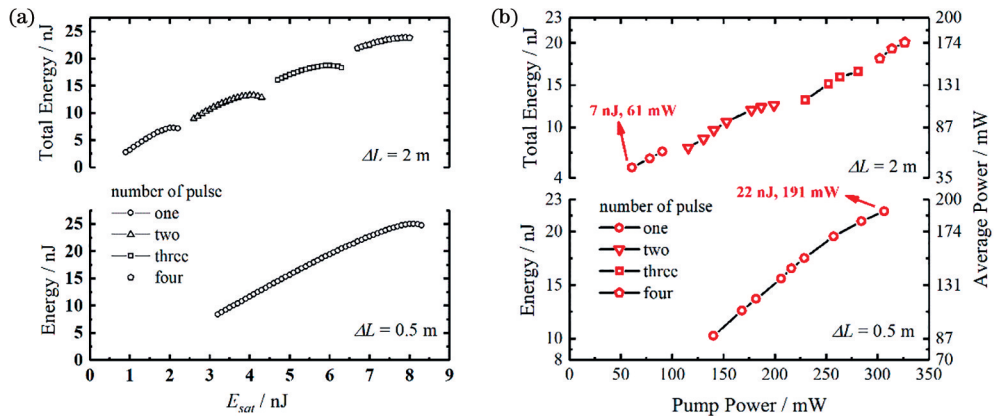


图 6 对脉冲分裂阈值的影响^[17]。(a) 不同 ΔL 的仿真结果;(b) 不同 ΔL 的实验结果

Fig. 6 Effect on pulse splitting threshold^[17]. (a)Simulated results at different ΔL ;

(b) experimental results at different ΔL

同年,清华大学^[46]在全正色散区域搭建了基于全保偏 NALM 环结构的耗散孤子共振锁模,如图 7(a)所示,整体腔长 80 m,重复频率为 2.59 MHz。

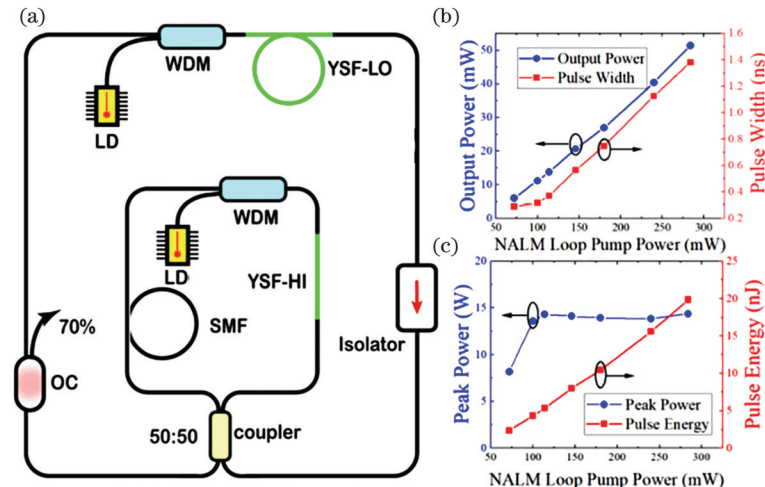


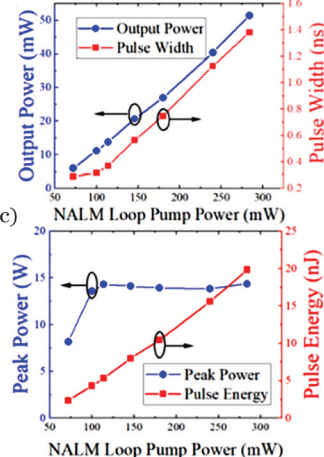
图 7 耗散孤子共振实验^[46]。(a)耗散孤子共振激光器示意图;(b)脉宽、功率与 NALM 环泵浦功率的关系;(c)能量、峰值功率与 NALM 环泵浦功率的关系

Fig. 7 Experiment on DSR^[46]. (a) Schematic of the DSR laser; (b) pulse width and output power versus NALM loop pump power; (c) pulse energy and peak power versus NALM loop pump power

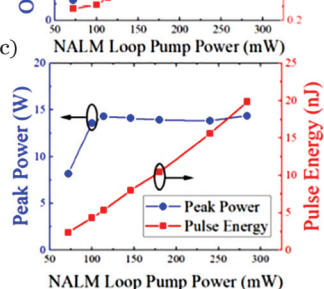
NALM 环的可饱和吸收效应对锁模状态的影响,仿真模拟了 NALM 环中增益光纤前后单模光纤长度差 ΔL 对脉冲分裂阈值的影响,如图 6 所示。在 $\Delta L=0.5 \text{ m}$ 和 $\Delta L=2 \text{ m}$ 时,模拟了输出能量和泵浦强度的关系,可以看出在 $\Delta L=0.5 \text{ m}$ 时,增益光纤位置对称性更高,所能实现的脉冲能量更高,可达 25 nJ 左右,而在 $\Delta L=2 \text{ m}$ 时,脉冲在 7 nJ 附近便开始分裂为多个脉冲,并随着泵浦强度的提升,脉冲数量也周期性增加,单脉冲能量始终限制在 10 nJ 以内。根据理论开展相关实验,根据图 6(b)可以看出,通过优化 NALM 环和泵浦参数,最终实现了脉冲能量为 22 nJ,重复频率为 8.7 MHz,平均功率高达 191 mW,脉冲宽度小于 200 fs 的输出。

改变 NALM 环中的泵浦功率可以实现脉宽 ps 到 ns 量级的调节范围,如图 7(b)所示。从图 7(c)可以看出,当泵浦功率超过 100 mW 时,峰值功率基

(b)



(c)



本维持不变,而脉冲能量可以继续提高,最高超过 20 nJ,实验中同时监测到了耗散孤子共振中的多脉冲现象。耗散孤子共振锁模激光器得益于直接输出脉冲能量高的优势,省去了预放大级,成本低廉,有着广阔的商业应用前景^[80]。然而,在大能量下脉冲宽度过宽,并且矩形脉冲的啁啾信息一般集中在两翼,中间啁啾量基本为零,导致无法使用常规色散补偿器件对其压缩^[81-82],脉宽很难达到飞秒量级。

另外,锁模光纤激光器本身是一个耗散系统,即使在具有全光纤锁模结构的振荡器中也会存在各种非稳态锁模状态^[83],如不稳定巨波^[84-85]、湍流^[86]、脉动^[87]、孤子分子^[88-89]等。近些年,研究者们借助色散傅里叶变换(DFT)技术^[90],详细地记录和刻画这些非稳态现象的非线性动力学过程,取得了丰富的研究成果,为人们对非线性科学的认知增添了许多新的见解,同时也为构建高稳定的激光振荡器提供了许多重要理论指导。

1994 年,Deissler 等理论上预测了耗散激光器中脉动孤子的存在^[91-92]。后来大量的理论和实验研究表明,非稳态锁模孤子如爆炸孤子、脉动孤子、脉动孤子分子等,广泛存在于各类锁模光纤振荡器中^[93-98]。2018 年,华中科技大学^[99]首次研究了基于 NPE 锁

模的正色散区域内脉动孤子的时空光谱动力学。同年,华南师范大学^[100]报道了负色散区域脉动孤子的混沌现象。2020 年,该组^[97]又报道了一种“不可见”脉动孤子,这种孤子的能量在时间上几乎恒定不变,但是光谱和脉冲形状呈周期性演变,意味着仅依据能量的波动无法判定激光器的锁模状态。同年,南开大学^[101]研究了基于 NPE 锁模的异步多孤子脉动现象,揭示了耗散激光振荡器中的多重稳定性,北京航空航天大学^[102]研究了基于单臂碳纳米管的锁模振荡器内的三种典型的脉动现象。2015 年,Runge 等^[103]首次报道了全保偏 NALM 全正色散激光器中的非稳定锁模——耗散孤子爆炸,如图 8(a)所示,在 100 个连续光谱中观测到了 7 个孤子爆炸。图 8(b)给出了爆炸区域的 4 个光谱,除了可以看到 1028 nm 附近光谱的坍塌重建,还可以看出孤子爆炸诱导 1075 nm 处拉曼光谱的产生。而准稳定区域没有这种拉曼光谱,意味着能量凝结成窄光谱时,成为有效的拉曼泵浦源。该组^[104]研究了腔内各参数(泵浦强度、主环无源光纤长度等)对孤子爆炸现象的影响,并证明了孤子爆炸存在于广泛的腔参数空间内。2018 年,Nazari 等^[94]理论上探索了孤子爆炸状态向稳态锁模孤子的转变途径。

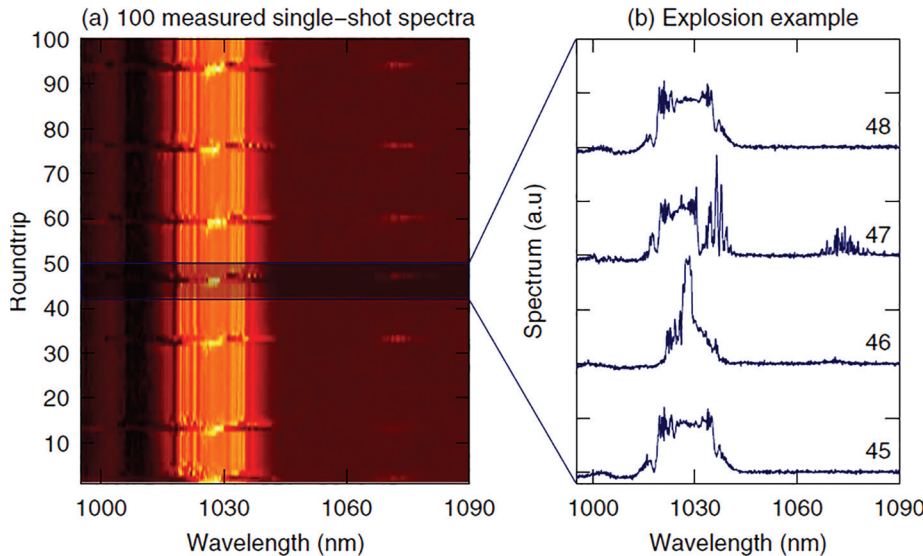


图 8 锁模光纤激光器中的孤子爆炸^[103]。(a) 连续光谱演化;(b) 特定圈数下的光谱图

Fig. 8 Soliton explosion in mode-locked fiber laser^[103]. (a) Continuous spectrum evolution; (b) spectrogram under certain number of cycles

同样,NALM 环锁模的全正色散激光器中也存在非稳定的脉动孤子锁模。2021 年,清华大学^[105]首次研究了脉动孤子起振的非线性动力学过程,实验光路如图 9(f)所示,借助 DFT 技术,记录了长短尺度下的物理图像,详细阐述了起振过程中的光谱、

能量以及峰值功率的演化。图 9(a)、(c)分别绘制了相应的脉冲强度和光谱带宽随圈数的变化。图 9(e)列举了过渡过程中一些代表性的归一化光谱。可以明显看出,光谱演化的 5 个特征阶段包括整形、展宽、振荡、窄化和稳定。整形阶段从第 5104 圈开

始,当脉冲达到孤子形成阈值能量时,腔内增益导致脉冲瞬态高峰值强度,由于强烈的非线性效应,形成超宽光谱,并在 5 圈演化之后,光谱整形为高斯形状,中心波长为 1030 nm,谱宽为 6 nm,如第 5108 圈光谱所示。这种前期光谱整形现象的出现,背后的原因可能是全正常色散腔内的带通滤波效应。接着受到自相位调制效应的影响,光谱在 3 圈演化中迅速展宽并形成典型的 M 形光谱,光谱边缘的一些尖峰是相位的不连续性引起的。在第 5114 圈,光谱明显变窄,这是由于加宽的光谱边缘分量承受了更多腔内带通滤波器和增益滤波效应引入的损耗。随后光谱再次展宽,光谱如此交替地展宽和窄化,意味着演化进入了振荡阶段,此阶段从第 5113 圈到第

5373 圈,持续 260 圈,如图 9(a)、(b)所示,脉冲强度和光谱带宽存在同步的剧烈振荡,这种振荡现象与腔内增益和损耗的瞬时失衡有关,脉冲强度的波动引起自相位调制强度的改变,从而导致光谱的同步变化。紧接着脉冲经历了 1400 圈的光谱窄化过程,同时伴随着强度的缓慢下降,如图 9(c)、(d)所示,这一阶段为脉冲的自组织过程,通过调整脉冲自身属性以适应激光腔的耗散参数,并最终转变为脉动孤子态。值得说明的是,作者进行了许多重复实验来记录脉动孤子的建立过程,发现这 5 个阶段及非稳调 Q 一直存在,说明这些过程在脉动孤子建立中并非偶然,将来更多的理论研究可能会为这种演变提供更多的见解。

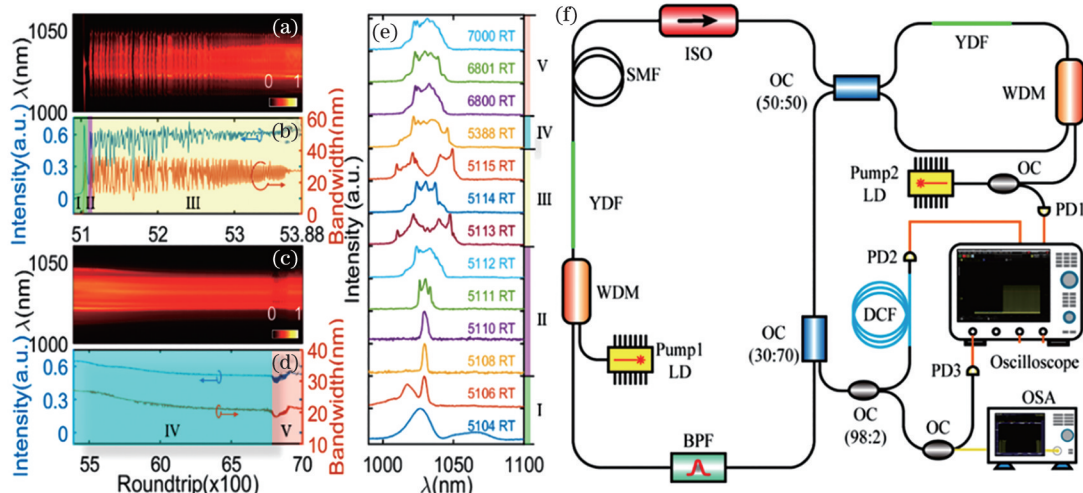


图 9 短时间尺度下脉动孤子形成的演化过程^[105]。(a)(c)DFT 记录的光谱演化;(b)(d)峰值功率与带宽演化;(e)特定圈数下的光谱;(f)实验光路

Fig. 9 Evolution of pulsating soliton formation in short time scale^[105]. (a)(c)Spectral evolution recorded by DFT; (b)(d)peak power and bandwidth evolution; (e) spectra under certain number of cycles; (f)experimental path

4 基于微纳光纤的锁模激光器

如前所述,色散管理也是锁模光纤激光器中重要的关键技术之一。尤其在色散管理孤子锁模与自相似孤子锁模中,均需要在腔内添加负色散元件,总色散量决定了超短脉冲的成型机制,对超短脉冲的光谱形状、脉冲宽度、脉冲能量、脉冲形成过程的瞬态物理效应、脉冲的噪声性能等都有着重要的影响。尽管自由空间光学元件[比如棱镜对、光栅对和吉莱-图努瓦干涉反射镜(GTI)]原则上可以实现任意波段的色散管理与补偿,然而它们体积较大,光路的对准和调节都不方便,降低了光纤激光器的稳定性和易用性。因此,全光纤色散管理技术一直受到较多关注。

对于 1.5 μm 波段,各种具有色散性能的光纤已有成熟的产品,比如普通单模光纤、色散补偿光纤

和高非线性光纤,分别具有负色散、正色散和近零色散。然而 1 μm 波段普通光纤均呈正色散,2 μm 波段普通光纤的色散又均为负,同时还有较大的三阶色散,因此如何利用与光纤系统兼容的方法在振荡器中补偿普通光纤的色散,形成性能优良的超短脉冲一直备受关注。

可对普通光纤进行熔融拉锥而方便地获得微纳光纤^[106-108],它的直径在波长量级,长度可达数十厘米。它的纤芯与空气包层间的折射率差很大,对模场的约束能力很强,因此在色散方面具有不同寻常的性质。通过控制微纳光纤的直径,可以在 1 μm 和 2 μm 波段分别获得较大的负色散和正色散,可用于超短脉冲光纤振荡器的色散管理,如图 10(a)与(b)所示。除了色散特性外,微纳光纤还具有很强的非线性效应,这是因为微纳光纤可以在数十厘

米的长度上始终将光约束在波长尺度，相对于普通光纤，有效非线性系数增加了 1~2 个量级，如图 10(c) 所示，因而微纳光纤可极大地增强腔内超短脉冲引起的非线性光学效应。不仅如此，微纳光纤本身的传输损耗极低，还可以通过绝热拉锥与普通光纤

不间断相连，从而使得它与普通光纤近乎无损耗连接。图 10(d) 表明，20 cm 长的直径为 1 μm 的微纳光纤在 1 μm 波段的插入损耗可低至 0.06 dB，因而微纳光纤接入谐振腔后并不会显著降低谐振腔的品质因子，获得高的腔内激光功率。

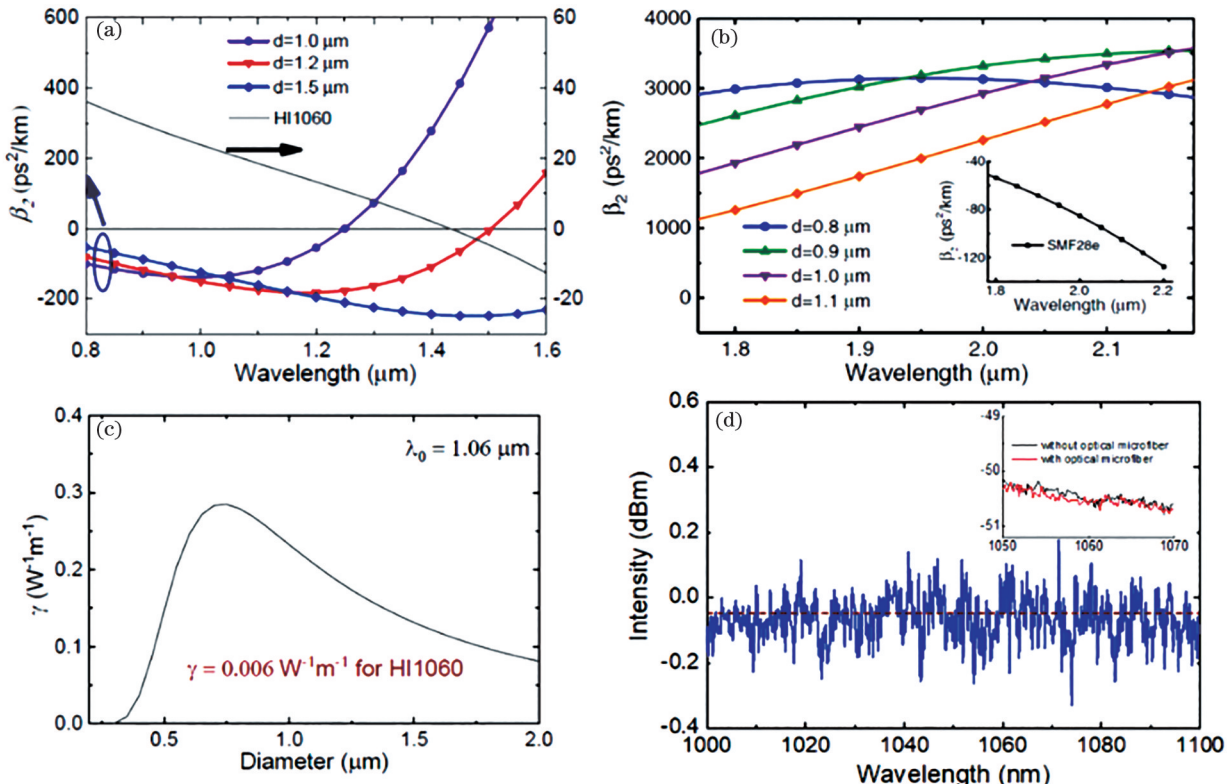


图 10 微纳光纤的属性^[106-108]。(a)(b)不同直径的微纳光纤在 1 μm 波段和 2 μm 波段的二阶色散；(c)不同直径微纳光纤的有效非线性系数；(d) 1 μm 直径微纳光纤的插入损耗

Fig. 10 Properties of microfiber^[106-108]. (a)(b) Calculated second-order dispersion of micro-nano fibers with different diameters at around 1 μm and 2 μm wavelength; (c) calculated effective nonlinear coefficient of micro-nano fibers with different diameters; (d) measured insertion loss of micro-nano fiber with a diameter of 1 μm

清华大学李宇航与浙江大学童利民教授合作，报道了 1 μm 和 2 μm 波段的基于微纳光纤的锁模激光器^[109-110]，证实了微纳光纤可用于 1 μm 波段和 2 μm 波段光纤激光器中色散管理，如图 11 所示。特别是在 2 μm 波段，微纳光纤的色散可达 2700 ps²/km，同时还具有很大且与普通光纤符号相反的三阶色散，因此可用于二阶和三阶色散的同时补偿。相比于微结构光纤（用于提供 1 μm 波段的负色散）和高数值孔径光纤（用于提供 2 μm 波段的正色散），微纳光纤具有色散可控、熔接方便、插入损耗低的优点。

除了色散补偿外，微纳光纤的高非线性系数会增强腔内超短脉冲的非线性效应，因而可用于超短脉冲振荡源。图 12(a)、(c) 为基于微纳光纤的掺 Yb 光纤振荡器的光路结构。掺 Yb 光纤振荡

器可以直接输出光谱范围为 1000~1600 nm 的超宽光谱，如图 12(b)、(d) 所示^[111]。基于微纳光纤的掺 Tm 光纤振荡器则可以直接输出光谱范围为 1600~2300 nm 的超宽谱类噪声，如图 12(e)~(g) 所示。不仅如此，微纳光纤中的模式色散会带来 2 μm 波段激光和其三倍频间的相位匹配，从而在产生超宽谱类噪声的同时，微纳光纤中还可以观察到三倍频，如图 12(h)、(i) 所示，这在其他光纤中是难以实现的^[112]。

微纳光纤的另一个特点是在微纳光纤周围存在较强的倏逝场，因此微纳光纤与低维材料构成的复合波导可以用作全光纤饱和吸收体，便于研究低维材料的饱和吸收性质，也被广泛用于光纤锁模激光器中。关于这一方面的研究进展可参见文献[113]，在此不再赘述。

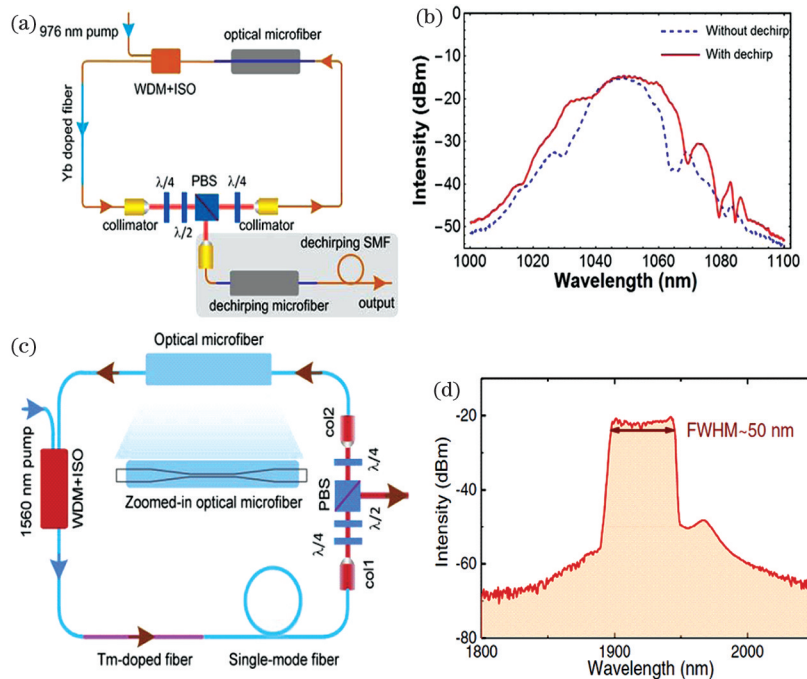


图 11 微纳光纤锁模光纤激光器^[109-110]。(a)(c) 1 μm 波段和 2 μm 波段基于微纳光纤的锁模激光器示意图；(b)(d) 超短脉冲的光谱

Fig. 11 Mode-locked fiber laser based on microfiber^[109-110]. (a)(c) Schematic of micro-nano fiber-based mode-locked fiber lasers with around 1 μm and 2 μm wavelength; (b)(d) corresponding spectra of ultrashort pulse

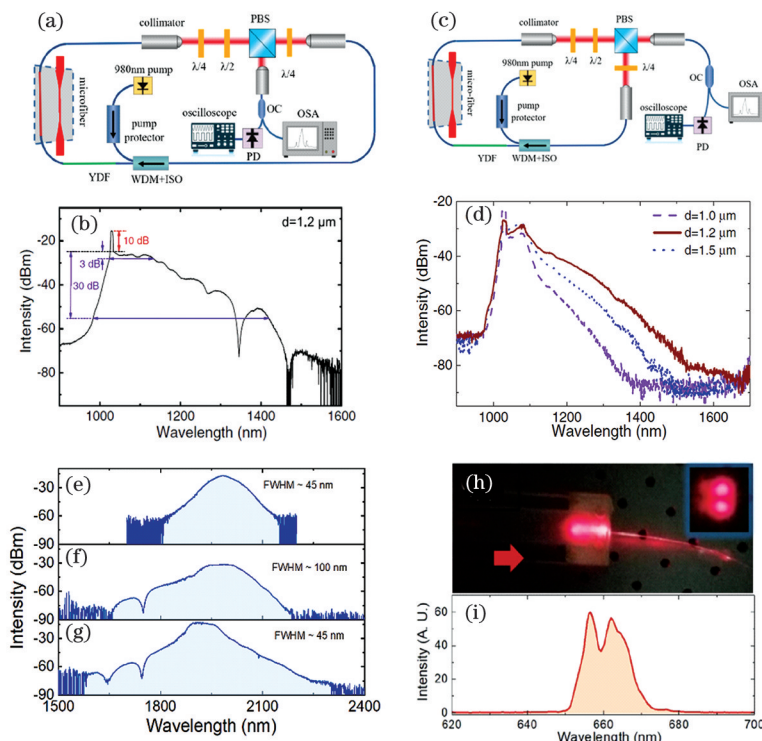


图 12 微纳光纤的其他激光器应用。(a)(c) 基于微纳光纤的掺 Yb 光纤振荡器的光路结构；(b)(d) 对应的 1 μm 波段类噪声光谱^[111]；(e)～(g) 在反射式输出光路中，微纳光纤调控 2 μm 波段的色散得到的类噪声光谱；(h)(i) 在微纳光纤中观察到的三倍频红光输出及其光谱^[112]

Fig. 12 Microfiber for other laser applications. (a)(c) Optical structure of Yb-doped fiber oscillator based on micro-nano fiber; (b)(d) corresponding 1 μm-band noise-like spectra; (e)–(g) in the reflective output optical path, noise-like spectra of 2 μm-band dispersion modulated by the micro-nano fiber; (h)(i) photograph and optical spectrum of simultaneous third harmonic generation in the micro-nano fiber

5 结 论

介绍了超快光纤振荡器中的各种锁模技术与结构,分析了各技术的优势与不足,并重点讨论了全光纤NALM环锁模振荡器和微纳光纤锁模振荡器的研究现状与发展趋势。不可否认,新型技术的出现和原有锁模技术的优化都极大地促进了锁模光纤激光器的发展。而激光器各种参数的提升与结构的改善,又不断地为各种科学和工业问题提供更优的解决方案。光纤激光器得益于本身结构紧凑、集成性高的优点,也是取代固体激光器的一种选择。在未来,锁模光纤激光器在满足应用需求的情况下,也将向着全光纤化、小型化、集成化的方向发展。可以预见,未来锁模光纤振荡器的发展仍将主要围绕全光纤化、大能量、窄脉宽等。同时新概念、新技术和新结构的不断出现,为飞秒光纤激光器的发展增光添彩,这些多元化技术的发展也必将为锁模光纤激光器提供更广阔的应用前景。

参 考 文 献

- [1] Dzhibladze M I, Ésiashvili Z G, Teplitskii É S, et al. Mode locking in a fiber laser[J]. Soviet Journal of Quantum Electronics, 1983, 13(2): 245-247.
- [2] Fermann M E, Hofer M, Haberl F, et al. Femtosecond fibre laser[J]. Electronics Letters, 1990, 26(20): 1737-1738.
- [3] Seise E, Klenke A, Limpert J, et al. Coherent addition of fiber-amplified ultrashort laser pulses[J]. Optics Express, 2010, 18(26): 27827-27835.
- [4] Keller U, Knox W H, Roskos H. Coupled-cavity resonant passive modelocked (RPM) Ti: sapphire laser[M]//Harris C B, Ippen E P, Mourou G A, et al. Ultrafast phenomena VII. Springer series in chemical physics. Heidelberg: Springer, 1990, 53: 69-71.
- [5] Zhou C, Yang W J, Zhang G X, et al. Novel ring cavity for ytterbium-doped mode-locked fiber laser incorporated with both SESAM and grating pair[J]. IEEE Photonics Technology Letters, 2009, 21(1): 3-5.
- [6] Tian X L, Tang M, Shum P P, et al. High-energy laser pulse with a submegahertz repetition rate from a passively mode-locked fiber laser[J]. Optics Letters, 2009, 34(9): 1432-1434.
- [7] Okhotnikov O, Grudinin A, Pessa M. Ultra-fast fibre laser systems based on SESAM technology: new horizons and applications [J]. New Journal of Physics, 2004, 6: 177.
- [8] Set S Y, Yaguchi H, Tanaka Y, et al. Laser mode locking using a saturable absorber incorporating carbon nanotubes [J]. Journal of Lightwave Technology, 2004, 22(1): 51-56.
- [9] Bao Q L, Zhang H, Wang Y, et al. Atomic-layer graphene as a saturable absorber for ultrafast pulsed lasers[J]. Advanced Functional Materials, 2009, 19(19): 3077-3083.
- [10] Hong S, Lédeé F, Park J, et al. Mode-locking lasers: mode-locking of all-fiber lasers operating at both anomalous and normal dispersion regimes in the C- and L-bands using thin film of 2D perovskite crystallites[J]. Laser & Photonics Reviews, 2018, 12(11): 1870050.
- [11] Woodward R I, Kelleher E J R. 2D saturable absorbers for fibre lasers[J]. Applied Sciences, 2015, 5(4): 1440-1456.
- [12] Liu W, Pang L, Han H, et al. 70-fs mode-locked erbium-doped fiber laser with topological insulator [J]. Scientific Reports, 2016, 6: 19997.
- [13] Fermann M E. Passive mode locking by using nonlinear polarization evolution in a polarization-maintaining erbium-doped fiber[J]. Optics Letters, 1993, 18(11): 894-896.
- [14] Doran N J, Wood D. Nonlinear-optical loop mirror [J]. Optics Letters, 1988, 13(1): 56-58.
- [15] Fermann M E, Haberl F, Hofer M, et al. Nonlinear amplifying loop mirror[J]. Optics Letters, 1990, 15(13): 752-754.
- [16] Jiang T X, Cui Y F, Lu P, et al. All PM fiber laser mode locked with a compact phase biased amplifier loop mirror[J]. IEEE Photonics Technology Letters, 2016, 28(16): 1786-1789.
- [17] Deng D C, Zhang H T, Gong Q H, et al. Energy scalability of the dissipative soliton in an all-normal-dispersion fiber laser with nonlinear amplifying loop mirror [J]. Optics & Laser Technology, 2020, 125: 106010.
- [18] Chédot C, Lecaplain C, Idlahcen S, et al. Mode-locked ytterbium-doped fiber lasers: new perspectives [J]. Fiber and Integrated Optics, 2008, 27 (5): 341-354.
- [19] Haus H A. Mode-locking of lasers[J]. IEEE Journal of Selected Topics in Quantum Electronics, 2000, 6(6): 1173-1185.
- [20] Ilday F O, Buckley J, Wise F W. Self-similar evolution of parabolic pulses in a fiber laser [C] // Nonlinear Guided Waves and Their Applications 2004, March 28-31, 2004, Toronto, Canada. Washington, D.C.: OSA, 2004: MD8.
- [21] Chong A, Renninger W H, Wise F W. Properties of

- normal-dispersion femtosecond fiber lasers [J]. Journal of the Optical Society of America B, 2008, 25(2): 140-148.
- [22] Mollenauer L F, Stolen R H, Gordon J P. Experimental observation of picosecond pulse narrowing and solitons in optical fibers[C]// Conference on Lasers and Electro-Optics 1981, June 10-12, 1981, Washington, D. C., United States. Washington, D.C.: OSA, 1981: WF1.
- [23] Kafka J D, Hall D W, Baer T. Mode-locked erbium-doped fiber laser with soliton pulse shaping [J]. Optics Letters, 1989, 14(22): 1269-1271.
- [24] Agrawal G P. Nonlinear fiber optics [M]. 5th ed. Amsterdam: Elsevier/Academic Press, 2013.
- [25] Nelson L E, Jones D J, Tamura K, et al. Ultrashort-pulse fiber ring lasers[J]. Applied Physics B, 1997, 65(2): 277-294.
- [26] Wu X, Tang D Y, Zhao L M, et al. Effective cavity dispersion shift induced by nonlinearity in a fiber laser [J]. Physical Review A, 2009, 80: 013804.
- [27] Tamura K, Ippen E P, Haus H A, et al. 77-fs pulse generation from a stretched-pulse mode-locked all-fiber ring laser[J]. Optics Letters, 1993, 18(13): 1080-1082.
- [28] Haus H A, Tamura K, Nelson L E, et al. Stretched-pulse additive pulse mode-locking in fiber ring lasers: theory and experiment[J]. IEEE Journal of Quantum Electronics, 1995, 31(3): 591-598.
- [29] Buckley J R, Wise F W, Ilday F Ö, et al. Femtosecond fiber lasers with pulse energies above 10 nJ[J]. Optics Letters, 2005, 30(14): 1888-1890.
- [30] Zhou X Y, Yoshitomi D, Kobayashi Y, et al. Generation of 28-fs pulses from a mode-locked ytterbium fiber oscillator[J]. Optics Express, 2008, 16(10): 7055-7059.
- [31] Tamura K, Haus H A, Ippen E P. Self-starting additive pulse mode-locked erbium fibre ring laser [J]. Electronics Letters, 1992, 28(24): 2226-2228.
- [32] Tamura K, Ippen E P, Haus H A. Pulse dynamics in stretched-pulse fiber lasers [J]. Applied Physics Letters, 1995, 67(2): 158-160.
- [33] Anderson D, Desaix M, Karlsson M, et al. Wave-breaking-free pulses in nonlinear-optical fibers [J]. Journal of the Optical Society of America B, 1993, 10(7): 1185-1190.
- [34] Nie B, Pestov D, Wise F W, et al. Generation of 42-fs and 10-nJ pulses from a fiber laser with self-similar evolution in the gain segment [J]. Optics Express, 2011, 19(13): 12074-12080.
- [35] Peacock A C, Kruhlak R J, Harvey J D, et al. Solitary pulse propagation in high gain optical fiber amplifiers with normal group velocity dispersion[J]. Optics Communications, 2002, 206(1/2/3): 171-177.
- [36] Soh D B, Nilsson J, Grudinin A B. Efficient femtosecond pulse generation using a parabolic amplifier combined with a pulse compressor II finite gain-bandwidth effect [J]. Journal of the Optical Society of America B, 2006, 23(1): 10-19.
- [37] Chong A, Buckley J, Renninger W, et al. All-normal-dispersion femtosecond fiber laser[J]. Optics Express, 2006, 14(21): 10095-10100.
- [38] Grelu P, Akhmediev N. Dissipative solitons for mode-locked lasers [J]. Nature Photonics, 2012, 6(2): 84-92.
- [39] Chong A, Renninger W H, Wise F W. All-normal-dispersion femtosecond fiber laser with pulse energy above 20 nJ[J]. Optics Letters, 2007, 32(16): 2408-2410.
- [40] Abdelalim M A, Logvin Y, Khalil D A, et al. Steady and oscillating multiple dissipative solitons in normal-dispersion mode-locked Yb-doped fiber laser [J]. Optics Express, 2009, 17(15): 13128-13139.
- [41] Zhang L Q, Pan Z Y, Zhuo Z, et al. Three multiple-pulse operation states of an all-normal-dispersion dissipative soliton fiber laser [J]. International Journal of Optics, 2014, 2014: 1-7.
- [42] Chang W, Ankiewicz A, Soto-Crespo J M, et al. Dissipative soliton resonances [J]. Physical Review A, 2008, 78(2): 023830.
- [43] Wu X, Tang D Y, Zhang H, et al. Dissipative soliton resonance in an all-normal-dispersion erbium-doped fiber laser[J]. Optics Express, 2009, 17(7): 5580-5584.
- [44] Luo Z C, Cao W J, Lin Z B, et al. Pulse dynamics of dissipative soliton resonance with large duration-tuning range in a fiber ring laser[J]. Optics Letters, 2012, 37(22): 4777-4779.
- [45] Semaan G, Braham F B, Salhi M, et al. Generation of high energy square-wave pulses in all anomalous dispersion Er : Yb passive mode locked fiber ring laser[J]. Optics Express, 2016, 24(8): 8399-8404.
- [46] Gong Q H, Zhang H T, Deng D C, et al. Dissipative soliton resonance in an all-polarization maintaining fiber laser with a nonlinear amplifying loop mirror [J]. IEEE Photonics Journal, 2020, 12(3): 1-8.
- [47] Krzempek K, Abramski K. Dissipative soliton resonance mode-locked double clad Er : Yb laser at different values of anomalous dispersion [J]. Optics Express, 2016, 24(20): 22379-22386.
- [48] Mei L, Chen G, Xu L, et al. Width and amplitude tunable square-wave pulse in dual-pump passively mode-locked fiber laser[J]. Optics Letters, 2014, 39

- (11): 3235-3237.
- [49] Guo B, Yao Y, Yang Y F, et al. Dual-wavelength rectangular pulse erbium-doped fiber laser based on topological insulator saturable absorber[J]. *Photonics Research*, 2015, 3(3): 94-99.
- [50] Zhao N, Liu M, Liu H, et al. Dual-wavelength rectangular pulse Yb-doped fiber laser using a microfiber-based graphene saturable absorber [J]. *Optics Express*, 2014, 22(9): 10906-10913.
- [51] Li D J, Tang D Y, Zhao L M, et al. Mechanism of dissipative-soliton-resonance generation in passively mode-locked all-normal-dispersion fiber lasers [J]. *Journal of Lightwave Technology*, 2015, 33 (18): 3781-3787.
- [52] Liu X M. Coexistence of strong and weak pulses in a fiber laser with largely anomalous dispersion [J]. *Optics Express*, 2011, 19(7): 5874-5887.
- [53] Fu W, Wright L G, Sidorenko P, et al. Several new directions for ultrafast fiber lasers [J]. *Optics Express*, 2018, 26(8): 9432-9463.
- [54] Pitois S, Finot C, Provost L, et al. Generation of localized pulses from incoherent wave in optical fiber lines made of concatenated Mamyshev regenerators [J]. *Journal of the Optical Society of America B*, 2008, 25(9): 1537-1547.
- [55] Liu Z W, Ziegler Z M, Wright L G, et al. Megawatt peak power from a Mamyshev oscillator[J]. *Optica*, 2017, 4(6): 649-654.
- [56] Liu W, Liao R Y, Zhao J, et al. Femtosecond Mamyshev oscillator with 10-MW-level peak power [J]. *Optica*, 2019, 6(2): 194-197.
- [57] Samartsev I, Bordenyuk A, Gapontsev V. Environmentally stable seed source for high power ultrafast laser [J]. *Proceedings of SPIE*, 2017, 10085: 100850S.
- [58] Regelskis K, Želudevičius J, Viskontas K, et al. Ytterbium-doped fiber ultrashort pulse generator based on self-phase modulation and alternating spectral filtering[J]. *Optics Letters*, 2015, 40(22): 5255-5258.
- [59] Sidorenko P, Fu W, Wright L G, et al. Multi-megawatt, self-seeded Mamyshev oscillator [C] // *Specialty Optical Fibers 2018*, Zurich, Switzerland. Washington, D.C.: OSA, 2018: SoM3H.4.
- [60] Woodward R I, Kelleher E J. Towards ‘smart lasers’: self-optimisation of an ultrafast pulse source using a genetic algorithm [J]. *Scientific Reports*, 2016, 6: 37616.
- [61] Pu G Q, Yi L L, Zhang L, et al. Intelligent programmable mode-locked fiber laser with a human-like algorithm[J]. *Optica*, 2019, 6(3): 362-369.
- [62] Li C, Ma Y, Gao X, et al. 1 GHz repetition rate femtosecond Yb: fiber laser for direct generation of carrier-envelope offset frequency[J]. *Applied Optics*, 2015, 54(28): 8350-8353.
- [63] Martinez A, Yamashita S. Multi-gigahertz repetition rate passively modelocked fiber lasers using carbon nanotubes [J]. *Optics Express*, 2011, 19 (7): 6155-6163.
- [64] Wang W L, Lin W, Cheng H H, et al. Gain-guided soliton: scaling repetition rate of passively modelocked Yb-doped fiber lasers to 12.5 GHz[J]. *Optics Express*, 2019, 27(8): 10438-10448.
- [65] Avdokhin A V, Popov S V, Taylor J R. Totally fiber integrated, figure-of-eight, femtosecond source at 1065 nm [J]. *Optics Express*, 2003, 11 (3): 265-269.
- [66] Szczepanek J, Kardaś T M, Michalska M, et al. Simple all-PM-fiber laser mode-locked with a nonlinear loop mirror[J]. *Optics Letters*, 2015, 40 (15): 3500-3503.
- [67] Nicholson J W, Ramachandran S, Ghalmi S. A passively-modelocked, Yb-doped, figure-eight, fiber laser utilizing anomalous-dispersion higher-order-mode fiber[J]. *Optics Express*, 2007, 15(11): 6623-6628.
- [68] Aguergaray C, Broderick N G R, Erkintalo M, et al. Mode-locked femtosecond all-normal all-PM Yb-doped fiber laser using a nonlinear amplifying loop mirror [J]. *Optics Express*, 2012, 20 (10): 10545-10551.
- [69] Erkintalo M, Aguergaray C, Runge A, et al. Environmentally stable all-PM all-fiber giant chirp oscillator[J]. *Optics Express*, 2012, 20(20): 22669-22674.
- [70] Aguergaray C, Hawker R, Runge A F J, et al. 120 fs, 4.2 nJ pulses from an all-normal-dispersion, polarization-maintaining, fiber laser [J]. *Applied Physics Letters*, 2013, 103(12): 121111.
- [71] Zhou J Q, Gu X J. 50.5 nJ, 750 fs all-fiber all polarization-maintaining fiber laser [C] // *CLEO: Science and Innovations 2015*, May 10-15, 2015, San Jose, California, United States. Washington, D.C.: OSA, 2015: SM3P.1.
- [72] Zhou J Q, Gu X J. 32-nJ 615-fs stable dissipative soliton ring cavity fiber laser with Raman scattering [J]. *IEEE Photonics Technology Letters*, 2016, 28 (4): 453-456.
- [73] Kuse N, Jiang J, Lee C C, et al. All polarization-maintaining Er fiber-based optical frequency combs with nonlinear amplifying loop mirror [J]. *Optics Express*, 2016, 24(3): 3095-3102.

- [74] Gao G, Zhang H T, Li Y H, et al. All-normal-dispersion fiber laser with NALM: power scalability of the single-pulse regime[J]. *Laser Physics Letters*, 2018, 15(3): 035106.
- [75] Yu Y, Teng H, Wang H B, et al. Highly-stable mode-locked PM Yb-fiber laser with 10 nJ in 93-fs at 6 MHz using NALM[J]. *Optics Express*, 2018, 26 (8): 10428-10434.
- [76] Shi Y H, Cheng Z C, Peng Z G, et al. Mode-locked fiber laser with a nonlinear amplifying loop mirror at different repetition rate varying from 100 kHz to 21 MHz[J]. *Proceedings of SPIE*, 2020, 11437: 114370L.
- [77] Aguergaray C, Runge A, Erkintalo M, et al. Raman-driven destabilization of mode-locked long cavity fiber lasers: fundamental limitations to energy scalability [J]. *Optics Letters*, 2013, 38 (15): 2644-2656.
- [78] Bednyakova A E, Babin S A, Kharenko D S, et al. Evolution of dissipative solitons in a fiber laser oscillator in the presence of strong Raman scattering [J]. *Optics Express*, 2013, 21(18): 20556-20564.
- [79] Runge A F J, de Aguergaray C, Provo R, et al. All-normal dispersion fiber lasers mode-locked with a nonlinear amplifying loop mirror[J]. *Optical Fiber Technology*, 2014, 20(6): 657-665.
- [80] Özgören K, Öktem B, Yilmaz S, et al. 83 W, 3.1 MHz, square-shaped, 1 ns-pulsed all-fiber-integrated laser for micromachining [J]. *Optics Express*, 2011, 19(18): 17647-17652.
- [81] Duan L N, Liu X M, Mao D, et al. Experimental observation of dissipative soliton resonance in an anomalous-dispersion fiber laser[J]. *Optics Express*, 2012, 20(1): 265-270.
- [82] Liu X M. Pulse evolution without wave breaking in a strongly dissipative-dispersive laser system [J]. *Physical Review A*, 2010, 81(5): 053819.
- [83] Martinez A, Sun Z P. Nanotube and graphene saturable absorbers for fibre lasers [J]. *Nature Photonics*, 2013, 7(11): 842-845.
- [84] Lecaplain C, Grelu P, Soto-Crespo J M, et al. Dissipative rogue waves generated by chaotic pulse bunching in a mode-locked laser[J]. *Physical Review Letters*, 2012, 108(23): 233901.
- [85] Dudley J M, Dias F, Erkintalo M, et al. Instabilities, breathers and rogue waves in optics[J]. *Nature Photonics*, 2014, 8(10): 755-764.
- [86] Turitsyna E G, Smirnov S V, Sugavanam S, et al. The laminar-turbulent transition in a fibre laser[J]. *Nature Photonics*, 2013, 7(10): 783-786.
- [87] Chen H J, Tan Y J, Long J G, et al. Dynamical diversity of pulsating solitons in a fiber laser [J]. *Optics Express*, 2019, 27(20): 28507-28522.
- [88] Krupa K, Nithyanandan K, Andral U, et al. Real-time observation of internal motion within ultrafast dissipative optical soliton molecules [J]. *Physical Review Letters*, 2017, 118(24): 243901.
- [89] Shi H S, Song Y J, Wang C, et al. Observation of subfemtosecond fluctuations of the pulse separation in a soliton molecule[J]. *Optics Letters*, 2018, 43 (7): 1623-1626.
- [90] Goda K, Jalali B. Dispersive Fourier transformation for fast continuous single-shot measurements [J]. *Nature Photonics*, 2013, 7(2): 102-112.
- [91] Akhmediev N, Soto-Crespo J M, Town G. Pulsating solitons, chaotic solitons, period doubling, and pulse coexistence in mode-locked lasers: complex Ginzburg-Landau equation approach [J]. *Physical Review E*, 2001, 63(5): 056602.
- [92] Soto-Crespo J M, Akhmediev N, Ankiewicz A. Pulsating, creeping, and erupting solitons in dissipative systems [J]. *Physical Review Letters*, 2000, 85(14): 2937-2940.
- [93] Du W X, Li H P, Li J W, et al. Vector dynamics of pulsating solitons in an ultrafast fiber laser [J]. *Optics Letters*, 2020, 45(18): 5024-5027.
- [94] Nazari S H, Arabanian A S. Comprehensive study of the transitions between stable mode-locking and soliton explosions in a fiber laser mode-locked with a nonlinear amplifying loop mirror[J]. *Journal of the Optical Society of America B*, 2018, 35 (10): 2633-2641.
- [95] Wang X Q, He J Y, Mao B W, et al. Real-time observation of dissociation dynamics within a pulsating soliton molecule [J]. *Optics Express*, 2019, 27(20): 28214-28222.
- [96] Du Y, Han M, Shu X. Dark solitons in the exploding pulsation of the bright dissipative soliton in ultrafast fiber lasers[J]. *Optics Letters*, 2020, 45(3): 666-669.
- [97] Liu M, Wei Z W, Li H, et al. Visualizing the “invisible” soliton pulsation in an ultrafast laser[J]. *Laser & Photonics Reviews*, 2020, 14(4): 1900317.
- [98] Liu X M, Yao X K, Cui Y D. Real-time observation of the buildup of soliton molecules [J]. *Physical Review Letters*, 2018, 121(2): 023905.
- [99] Du Y, Xu Z, Shu X. Spatio-spectral dynamics of the pulsating dissipative solitons in a normal-dispersion fiber laser[J]. *Optics Letters*, 2018, 43 (15): 3602-3605.
- [100] Wei Z W, Liu M, Ming S X, et al. Pulsating soliton with chaotic behavior in a fiber laser [J]. *Optics*

- Letters, 2018, 43(24): 5965-5968.
- [101] Wang X Q, He J Y, Shi H M, et al. Real-time observation of multi-soliton asynchronous pulsations in an L-band dissipative soliton fiber laser [J]. Optics Letters, 2020, 45(17): 4782-4785.
- [102] Chen J, Zhao X, Li T, et al. Generation and observation of ultrafast spectro-temporal dynamics of different pulsating solitons from a fiber laser [J]. Optics Express, 2020, 28(9): 14127-14133.
- [103] Runge A F J, Broderick N G R, Erkintalo M. Observation of soliton explosions in a passively mode-locked fiber laser [J]. Optica, 2015, 2(1): 36-39.
- [104] Runge A F J, Broderick N G R, Erkintalo M. Dynamics of soliton explosions in passively mode-locked fiber lasers [J]. Journal of the Optical Society of America B, 2016, 33(1): 46-53.
- [105] Deng D C, Zhang H T, Zu J Q, et al. Buildup dynamics of a pulsating dissipative soliton in an all-normal-dispersion PM Yb-doped fiber laser with a NALM [J]. Optics Letters, 2021, 46(7): 1612-1615.
- [106] Tong L M, Gattass R R, Ashcom J B, et al. Subwavelength-diameter silica wires for low-loss optical wave guiding [J]. Nature, 2003, 426(6968): 816-819.
- [107] Brambilla G, Xu F, Horak P, et al. Optical fiber nanowires and microwires: fabrication and applications [J]. Advances in Optics and Photonics, 2009, 1(1): 107-161.
- [108] Li Y H, Zhao Y Y, Wang L J. Demonstration of almost octave-spanning cascaded four-wave mixing in optical microfibers [J]. Optics Letters, 2012, 37(16): 3441-3443.
- [109] Wang L, Xu P, Li Y, et al. Femtosecond mode-locked fiber laser at $1\text{ }\mu\text{m}$ via optical microfiber dispersion management [J]. Scientific Reports, 2018, 8(1): 4732.
- [110] Li Y H, Wang L Z, Kang Y, et al. Microfiber-enabled dissipative soliton fiber laser at $2\text{ }\mu\text{m}$ [J]. Optics Letters, 2018, 43(24): 6105-6108.
- [111] Zhou J, Li Y H, Ma Y G, et al. Broadband noise-like pulse generation at $1\text{ }\mu\text{m}$ via dispersion and nonlinearity management [J]. Optics Letters, 2021, 46(7): 1570-1573.
- [112] Li Y H, Kang Y, Guo X, et al. Simultaneous generation of ultrabroadband noise-like pulses and intracavity third harmonic at $2\text{ }\mu\text{m}$ [J]. Optics Letters, 2020, 45(6): 1583-1586.
- [113] Li Y H, Wang L Z, Li L J, et al. Optical microfiber-based ultrafast fiber lasers [J]. Applied Physics B, 2019, 125(10): 192-202.

Research Status of Mode-Locked Laser Based on Nonlinear Amplified Loop Mirror and Micro-Nano Fiber

Zhang Haitao^{*}, Deng Decai, Li Yuhang^{**}, Zu Jiaqi, Chen Junyu, Gong Mali, Liu Qiang

Key Laboratory of Photonic Control Technology, Ministry of Education, Center for Photonics and Electronics,

Department of Precision Instrument, Tsinghua University, Beijing 100084, China

Abstract

Significance Since the invention of the fiber laser is more than half a century ago, the performance index of fiber beam output has continuously improved, which is mainly reflected in the improvement of output pulse power, shortening of output pulse width, improvement of beam quality, and shaping of the laser spectrum. Femtosecond fiber laser, as an important branch of the fiber laser field, has been widely used in the industry, mainly because of its advantages over solid-state femtosecond lasers in the following three aspects. 1) All-optical slimming and high optical efficiency. Because of the pump light in the optical fiber waveguide transmission, the effective action distance is longer, which improves the conversion efficiency. Additionally, the fiber has the advantages of soft and easy-to-coil integration, so it can be connected through the welding process. 2) Close to the diffraction limit of the beam quality and good heat dissipation. As the signal light is confined to the optical fiber waveguide in the single-mode form, the output from the photonic crystal fiber with a large mode field diameter and chirality coupling optical fiber can help maintain a good speckled pattern. Additionally, the large cooling area of the heating effect of the solid gain medium can help overcome the inherent effect. It is an important way to realize high-power laser. 3) The ion emission spectrum in the fiber is wider, so that the fiber laser can achieve the output pulse with a narrower pulse width and a wider spectral width. Thanks to the ultra-short pulse width, ultra-wide spectrum, and ultra-high peak power of the

fiber laser, it has wide application prospects in industrial processing, communication detection, biological medicine, high-energy physics, material preparation, and chemistry, and other fields.

High energy, narrow pulse width, high stability of ultra-short pulses are also being researched throughout the optical fiber mode-locked oscillator development. Therefore, new principles, new technologies, and a variety of new laser materials have been revealed at historic moments, from active to passive mode-locking, from small energy width with a broad pulse width to high energy with a narrow pulse width, from a space structure to an all-fiber structure, from theoretical research to practical applications. In the past several decades, the fiber mode-locked oscillator has undergone rapid and comprehensive development, which has greatly promoted the development of new research fields and industrial markets. Now, the fiber mode-locked oscillator has become one of the core members of the laser family.

Progress Development of a fiber mode-locked oscillator revolves mainly around two themes. One theme involves a narrow pulse width and large energy in two main directions. One direction is based on theoretical study and is given priority to explore a new type of mode-locking mechanism. In this direction, it has experienced the traditional soliton, dispersion-management soliton, self-similar soliton, dissipative soliton resonance, and Mamyshev mode-locked soliton. The other direction is based on the use of new laser materials, including a new optical fiber, pump source, saturable absorption materials, and so on. To realize the all-optical fiber integration of the oscillator, adopting a special fiber structure is generally not suitable and realizing self-starting using the Mamyshev mode-locking is difficult; therefore, the nonlinear polarization evolution (NPE)-based all normal dispersion mode-locked oscillator is still the mainstream trend. NPE mode-locking can achieve a high single-pulse energy and a narrow pulse width. However, a polarization controller is necessary to adjust the cavity polarization state. Introducing a mechanical structure makes this type of oscillator sensitive to the environment, and ensuring the long-term stable mode-locking state is difficult. The mode-locked laser based on nonlinear amplified loop mirror (NALM) is the best choice for all-fiber integration. Such an oscillator can be used for all polarization-maintaining devices, which effectively avoid mode-locked dependence on the mechanical structure and have high environmental stability and reliability. Additionally, its output is linearly polarized—used as a CPA system of the seed source—and it can achieve high compression efficiency using a grating pair. However, when the femtosecond pulse is directly output by the oscillator, the dispersion management in the cavity becomes critical, especially in the 1- μm band. Because of a lack of negative dispersion devices, construction of such lasers becomes more difficult. Recently, the microfiber has injected new vitality in femtosecond fiber lasers. Therefore, we will review the development of these two types of mode-locked fiber oscillators herein.

Conclusion and Prospect Mode-locked fiber lasers are gradually becoming a powerful tool in many fields. High-energy and highly stable oscillators based on all-fiber structures are more attractive; among these, NALM and microfiber laser have undergone rapid development recently. However, the stability, reliability, and startup performance of these lasers need more detailed research to ensure their wider commercial use.

Key words laser technique; mode-locked fiber laser; nonlinear amplified loop mirror; micro-nano fiber; dissipative soliton; pulsating soliton

OCIS codes 140.4050; 140.3510; 140.7090